Peer-reviewed version available at Metals 2017, 7, , 152; doi:10.3390/met7050152

Aluminum Wires have the Free Air Balls (FABs): Electronic Flame-Off, Fracture Strength, Electrical Properties and Bonding Characteristics of Nano Zn Film Al-Si Bonding Wires

Fei-Yi Hung*, Truan-Sheng Lui, Kuan-Ming Chu, Yi-Wei Tseng

Department of Materials Science and Engineering, National Cheng Kung University, Tainan 701, TAIWAN.
Corresponding author. Tel.: +886-6-2757575-62950
Email: fyhung@mail.ncku.edu.tw (F.Y. Hung)

Abstract

Aluminum wire is a common material for wire bonding due to its resistance to oxidation and low price. It does not melt when becoming a free air ball (FAB) during the electronic flame-off (EFO) process with wettability, and is applied by wedge bonding. This study used 20μm Zn-Coated Al-0.5wt.%Si (ZAS) wires to improve the FAB shape after the EFO process, while maintaining stability of the mechanical properties, including the interface bonding strength and hardness. In order to test circuit stability after ball bonding, the current-tensile test was performed. During the experiment, it was found that 80nm ZAS with wire bonding has lower resistance and higher fusing current. For the bias tensile test, the thicker Zn film diffused into the Al-Si matrix easily, after which the strength was reduced. The ball-bond interfaces had no change in their condition before and after the bias. Accordingly, ZAS could be a promising candidate for ball bonding in the future.

Keywords: Al wire, free air ball (FAB),electronic flame-off (EFO), coating, bias test

1. Introduction

Al wire has been used in the wire-bonding process for decades; however, the percentage is relatively low compared to gold and copper wires because of its poor FAB shape and structure [1-2]. In addition, high or low wire resistance does not affect the functioning of an IC chip when the internal resistance of the whole IC chip (on-chip) is high. In other words, regardless of whether gold wire (low resistance) or gold alloy wire (high resistance) is used, similar resistance with the same IC chip results. Every bonding wire has its resistivity [3] (Au: 2.44×10^{-8}, Cu: 1.68×10^{-8}, and Al: 2.82×10^{-8}). However, after bonding, the resistances of the on-chip interconnects have almost identical resistivities. The reason is that the resistances of the bonding interfaces in the chip are high. For example, the resistance of the IMCs between the solder and copper pad is much higher than the resistance of the wires [4-5]. High purity Al wire has low resistance, and by adding 0.5wt.% Si, the mechanical properties can be improved without enhancing the resistance of the Al wire [6]. Melted Al oxidizes easily and results in poor ball morphology (i.e. can not form a FAB). In this study, we coated a Zn nano-film on the surface

Peer-reviewed version available at Metals 2017, 7, , 152; doi:10.3390/met7050152

of the Al-0.5Si wire to improve the EFO process. The reason we chose Zn is that its melting point and boiling temperature are both lower than Al, the latter of which is about 907℃. Due to these differences, a stable Al-Si-Zn FAB matrix can be obtained because Zn can protect Al from oxidation during the EFO process [7]. Accordingly, to better characterize this material, the mechanical and electrical properties after the Zn nano-film coated Al wire (ZAS) wire bonding are discussed in the present paper. Results indicate that the ZAS wire is suitable for ball bonding and that the presented EFO process could be used as a reference for packaging applications.

2. Experiment

In this study, the diameter of the employed fine Al-0.5Si wire was 20 μm, and was coated with a Zn nano-film by a chemical plating method, called electroless plating. The chemical plating solution included ZnO, NaOH, $KNaC_4H_4O_6 \cdot 4H_2O$ and water. Two coating thicknesses of the Zn thin film were obtained, namely 80nm (ZAS80) and 250nm (ZAS250), as shown in **Fig. 1**.

A free air-ball (FAB) was formed by the electronic flame-off (EFO) process with a wire-bonding machine (55mA, 15ms), the first FAB bond of which was on 800nm aluminum pads [8-9]. To prevent oxidation, a 95% nitrogen-5%

hydrogen gas mixture was used during the EFO process. Morphology and cross section analyses were performed by FIB-SEM. An Electron Probe X-ray Micro-analyzer (EPMA) was used to observe the element distribution in the Al-0.5Si wire. The hardness from the FAB to the wire was investigated by micro-hardness (HK), for which the loading force and holding time were 10gf and 10 sec, respectively. The pull test of the first bond was performed with a test length of 50 mm, yielding a strain rate of 5 x $10^{-3}s^{-1}$. Moreover, to better understand the differences between the Al-0.5Si and ZAS wires, current tests of the first bond (FAB) were compared [10-14] and the bias-tensile test of the wires with different currents was measured. The schematic diagram in **Fig. 2** shows that for the current test, the effective wire length was 30 mm, and the applied DC voltage was increased 0.05V/sec from 0V until the wire fused. In addition, the second bond specimens were compared before and after 48hr aging in a vacuum. All data are the average of 3-5 experimental repetitions.

3. Results and discussion

Fig. 3 shows the FIB-SEM images of the FABs from the two ZAS wires, including surface morphology and cross section. As can be seen, different Zn film thicknesses apparently affected the FAB morphology, degree of surface

Peer-reviewed version available at Metals 2017, 7, , 152; doi:10.3390/met7050152

roughness and cross-sectional structure.

The FAB surface and cross section images of the ZAS80, which were cut vertically, are shown in **Figs. 3a** and **b,** respectively. The image shows that the morphology of ZAS80 FAB was a circle, and that Zn apparently improved the shape of the Al-0.5Si FAB. Due to the lower Gibb's free energy of ZnO, formation of Al_2O_3 is hindered, resulting in a better FAB shape (**Fig. 3a**) [7].The dark spots on the surface of the FAB are pollutants. After the EFO process, observations of the FAB surface were performed immediately before more pollutants (induced air sulfide) had time to form on the surface. Further, micro-pores formed randomly due to the strong oxidation-reduction reaction and are visible in the FAB cross section (**Fig. 3b**) . This means that gas in the melting Al-0.5Si FAB could not be fully exhausted with the 80nm Zn coating on the surface [15]. Notably, previous research regarding powder sintering also found that zinc particles easily formed pores in liquid pools [16], as with our results. In order to improve this, we increased the thickness of the Zn film to 250nm (ZAS250), the morphology of which is shown in **Fig. 3c**. As seen, although the ZAS250 FAB surface was rough due to the strong oxidation-reduction reaction, there are no pores visible in the cross section image (**Fig. 3d**). This suggests that although a sufficient zinc content had an exhaust effect for the FAB, the

thicker zinc coating caused a rougher ball surface. The main reason is that Zn can protect Al from oxidation and lower the melting point during the EFO process.

The element distribution of ZAS250 after the EFO process is shown in **Fig. 4**. During EPMA analysis, the long scanning time on the ball zone caused some deformation in the ball portion. Actually, the as-received wire was an aluminum wire containing 0.5 wt.% Si, so there were some Si signals in the wire. A trace Zn signal was detected from the FAB to the heat-affected zone (HAZ: un-melted and solid-state surface reaction only); however, the signal became clear 100μm away from the FAB. The boiling point of Zn is 907℃, but the temperature of the EFO process is much higher; accordingly, Zn in the FAB and HAZ volatilized easily during the EFO process. In addition, adding Zn into the Al matrix can lower the alloy's melting point. As such, the gas in the ZAS250 FAB readily exhausted and caused a rougher FAB surface morphology. After the EFO process, we found: 1) Al wire without Zn coating can not form a FAB; 2) with 80nm Zn coating, the ball surface was smooth, but had pores inside the ball; and, 3) with 250nm Zn coating, the surface was rough, but the ball had no pores.

The micro-hardness and tensile properties of the ZAS80 wire after the EFO

process are shown in **Fig. 5**, which reveals that the neck of the FAB was the weakest. The hardness of the FAB center and the wire were about the same (**Fig. 5a**). This phenomenon can be attributed to the coarse grains in the neck of the FAB (HAZ area), which caused the low hardness [17-18]. After bonding on the Al pads, the breaking load of the ZAS80 and ZAS250 wires were found to both be about the same at 3.6gf, as presented in **Fig. 5b** (an image of the first bond is shown). This implies that neither the thickness of the Zn film nor the pores in the ZAS80 FAB had any effect on the bonding strength of the wires However, the coated Zn film for EFO did cause some effects in the FAB and HAZ: 1) the FAB had a lower melting point (re-melting and then solidification), increased wettability (form a ball), and easy gas exhaustion; and, 2) the HAZ (near neck zone) featured un-melted solid-state surface reactions only. The coated Zn film vaporized, and so no Zn signal was detected on the wire's surface.

ZAS wires used in wire bonding with ball bonding is an important innovation in packaging; consequently, investigating the electrical properties after wire bonding is necessary. The original wire (AS) without the coated Zn film could not achieve a good shape, so the current test with the wedge-bonding process was necessary. The experimental data for the fusing currents of the Al-0.5Si,

ZAS80 and ZAS250 wires are shown in **Fig. 6**. As can be seen, the I-V curves indicate that the three wires were all linear under 0.20A (zone I); however, resistances of the Zn-coated wires were reduced due to the oxidation prevention of the Zn film on the surface. When the current exceeded 0.20A (zone II), the wires' resistances greatly increased due to the joule heating of thermoelectricity. The resistances increased rapidly in tandem with the increasing current until fusing. The Al-0.5Si wire (not Zn coated) with wedge bonding had the highest fusing current of almost 0.3A, while the fusing currents of the ZAS80 and ZAS250 were 0.28 A and 0.26A, respectively. With the thinner Zn film (high purity), the ZAS80 wire had a lower resistance than the ZAS250; however, the latter had a lower fusing current due to the melting point being reduced by the higher Zn content. Notably, the pores in the ZAS80 FAB did not apparently influence the resistivity. Al metal has a high ductile property, but its FAB is a rapidly solidified structure with lower toughness. It was noted that the porous FAB of the ZAS80 wire had good ductility-toughness (sponge like) for wire bonding [19-20]. After bonding, the ZAS80 FABs processed a uniform deformation behavior. Accordingly, it is clear that a porous ball bond did not influence the stress concentration to reduce the interface strength.

Figure 7 shows the bias-tensile properties of the three wires with different

Peer-reviewed version available at Metals 2017, 7, , 152; doi:10.3390/met7050152

currents. The AS wire and ZAS80 wire featured bias-tensile strength of more than 9g in 0.15A, but that of the ZAS250 wire was lower. The main reason is that the thicker Zn film easily diffused into the Al-Si matrix under the Joule effect (from the surface into the core, thereby affecting the dispersion strengthening of Si), which reduced the strength. When increasing the current to more than 0.2A, the strength of the wires was decreased under the bias tensile test.

In **Figs 8-9**, the bonding Interfaces of the ZAS80 were observed before and after bias (60% fusing current for 24 hr). As shown, their interfaces are flat and no IMC formed. Consequently, it is clear that the interface resistance of ZAS80 is stable, and that the Al wire ball bonds on the Al pad possess good reliability.

After 48hr vacuum aging, the second bonds of the AS and ZAS80 wire were compared. This study used the nozzle of a gold-wire machine to perform the second current bonding, for which all specimens used the same bonding conditions. There are two reasons for this direct comparison: 1) to investigate whether the Zn coating can improve the bond-strength before heat aging and, 2) to check if the bond-interface peeled after heat aging. Due to the Al pad being a sputtered film and processes an obvious indentation. It was found that the appearance of the AS wire was similar before and after aging (**Fig. 10**). Notably,

the second bonds of the ZAS80 wire not only had good aging resistance (**Fig.11**), but also higher average pull-strength (the second bond strength, ZAS80=5.32g, AS=5.08g).In **Figs 10-11** present images of the second bond of the ball bonding machine for Al wire. In addition, the annealed Al pad is softer and causes a deeper indentation. Without pressing deeper, the ball-bond nozzle can not smoothly cut off the Al wire.

In this system (**Fig. 12**), the ZAS80 wire was found to be highly reliable for wire bonding; and in future studies, the bonding interface and aging characteristics for Al wire application will be investigated.

4. Conclusion

1) Currently, Al wires can not be used in wire bonding with ball bonding; however, coating Al-0.5Si wire with a Zn film can improve this problem. Further, the mechanical properties, bonding strengths and bias tensile strength of the ZAS wires are stable.

2) Pores in the ZAS80 wire FAB have no influence on bonding characteristics. Moreover, the low interface resistance and high fusing current of the ZAS80 wire hold potential for application in IC packaging.

Acknowledgements

The authors are grateful to the Instrument Center of National Cheng Kung University and the National Science Council of Taiwan (MOST 105-2628-E-

006-001-MY2) for their financial support.

Reference

1. M. S. Broll, U. Geissler, J. Höfer, S. Schmitz, O. Wittler, K. D. Lang, Microelectronics Reliability 55 (2015) 961-968.

2.S. Park, S. Nagao, T. Sugahara, K. Suganuma, Japanese Journal of Applied Physics 53 (2014) 069201.

3.http://chemistry.about.com/od/moleculescompounds/a/Table-Of-Electrical-Resistivity-And-Conductivity.htm

4. M. A. A. MohdSalleh, S. D. McDonald, H. Yasuda, A. Sugiyama, K. Nogita' ScriptaMaterialia 100 (2015) 17-20.

5. K. J. Chen, F. Y. Hung, T. S. Lui, L. H. Chen, D. W. Qiu, T. L. Chou, Microstructure and electrical mechanism of Sn-xAg-Cu PV-ribbon for solar cells, Microelectronic Engineering 116 (2014)33-39.

6.Y. Alemdag, M. Beder, Materials and Design 63 (2014) 159-167.

7. Y. Gencer, A. EmreGulec, Journal of Alloys and Compounds 525 (2012) 159-165.

8.H. W. Hsueh, F. Y. Hung, T. S. Lui, L. H. Chen, K. J. Chen, Advances in Materials Science and Engineering (2014) 925768.

9. Y. W. Tseng, F. Y. Hung, T. S. Lui, Microelectronics Reliability 55 (2015) 608-612.

10.Y. W. Tseng, F. Y. Hung, T. S. Lui, Microelectronics Reliability, 55(2015) 1256-1261.

11. K. J. Chen, F. Y. Hung, T. S. Lui, S. J. Chang, Z. S. Hu, Journal of Nanomaterials, (2012)272387.

12. H. W. Hsueh, F. Y. Hung, T. S. Lui, L. H. Chen, Microelectronics Reliability,

51(8) (2013) 1159-1163.

13. H. W. Hsueh, F. Y. Hung, T. S. Lui, L. H. Chen, K. J. Chen, Advances in Materials Science and Engineering, 2014, 925768, 6 pages.

14. Y. W. Tseng, F. Y. Hung, T. S. Lui, Journal of electronic materials (JEM), 45, (2016) 624-630.

15. W. S. Olivia, X. Liang, P.George, C. Orkid, J BiolInorgChem 17 (2012) 927-938

16. R. N. Lumley, G. B. Schaffer, Metallurgical and Materials Transactions A, 30A (1999) 1682-1685.

17.F. Y. Hung, Y. T. Wang, L. H. Chen, T. S. Lui, Materials Transactions 47 (2006) 1776-1781.

18.I. T. Huang, F. Y. Hung, T. S. Lui, L. H. Chen, H. W. Hsueh, *Microelectronics Reliability* 51 (2011) 25-29.

19. K. S. Zhang, J. B. Bai, D. Francžois, International Journal of Solids and Structures 36 (1999) 3407-3425.

20.F. Y. Hung, L. H. Chen, T. S. Lui, Wear 252 (2002) 985-991.

Peer-reviewed version available at Metals 2017, 7, , 152; doi:10.3390/met7050152

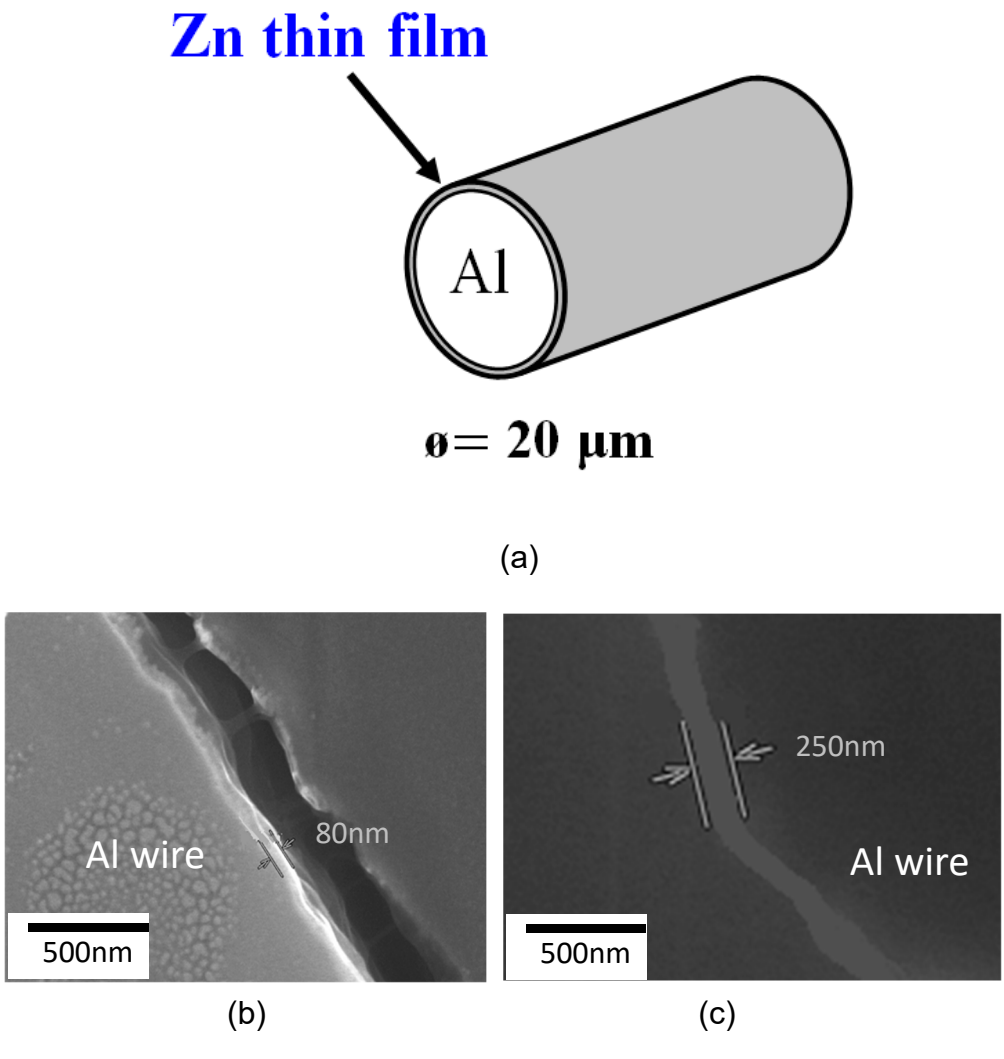

Figure 1(a) Schematic diagram of Zn-coated Al-0.5wt.% Si (ZAS) wire.

Cross-sections of (b) ZAS80 and (c) ZAS250 wire.

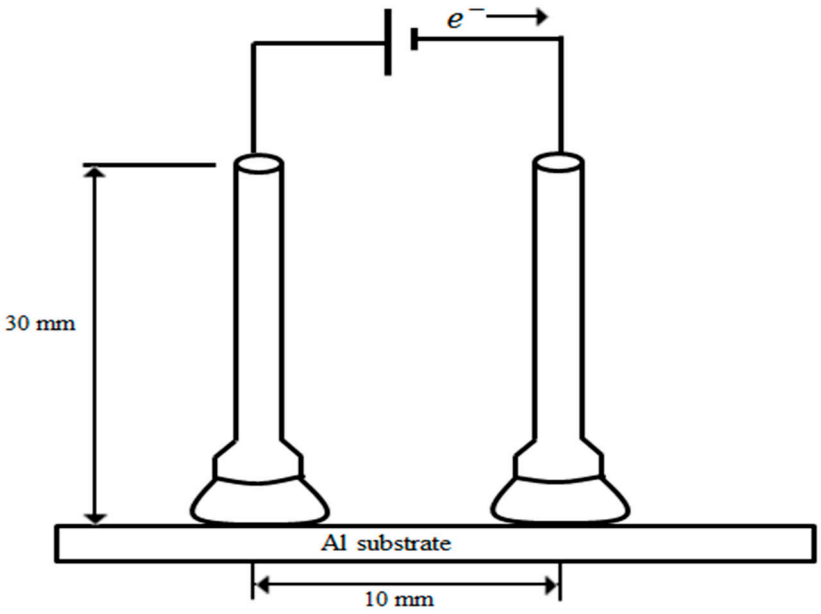

Figure 2 Schematic diagram of the bias test system.

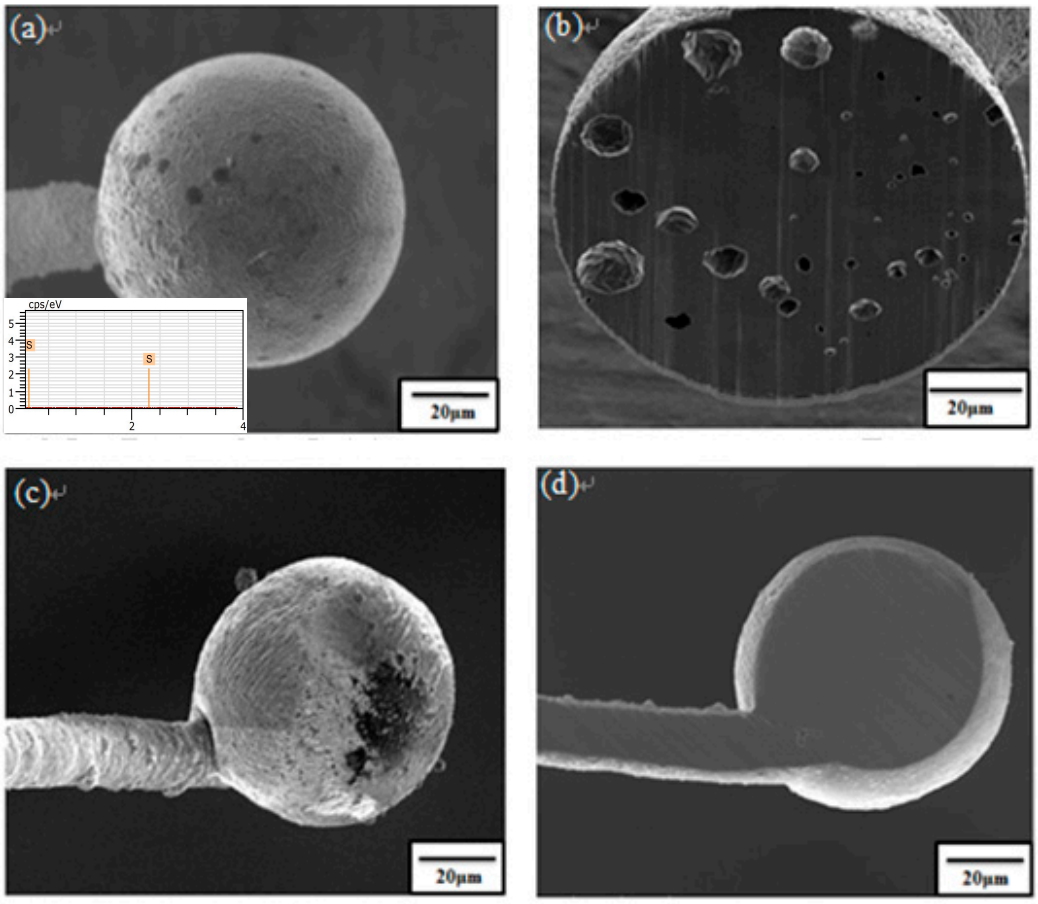

Figure3 Surface and cross-sectional images of the FABs: (a-b) ZAS80 wire; and, (c-d) ZAS250 wire.

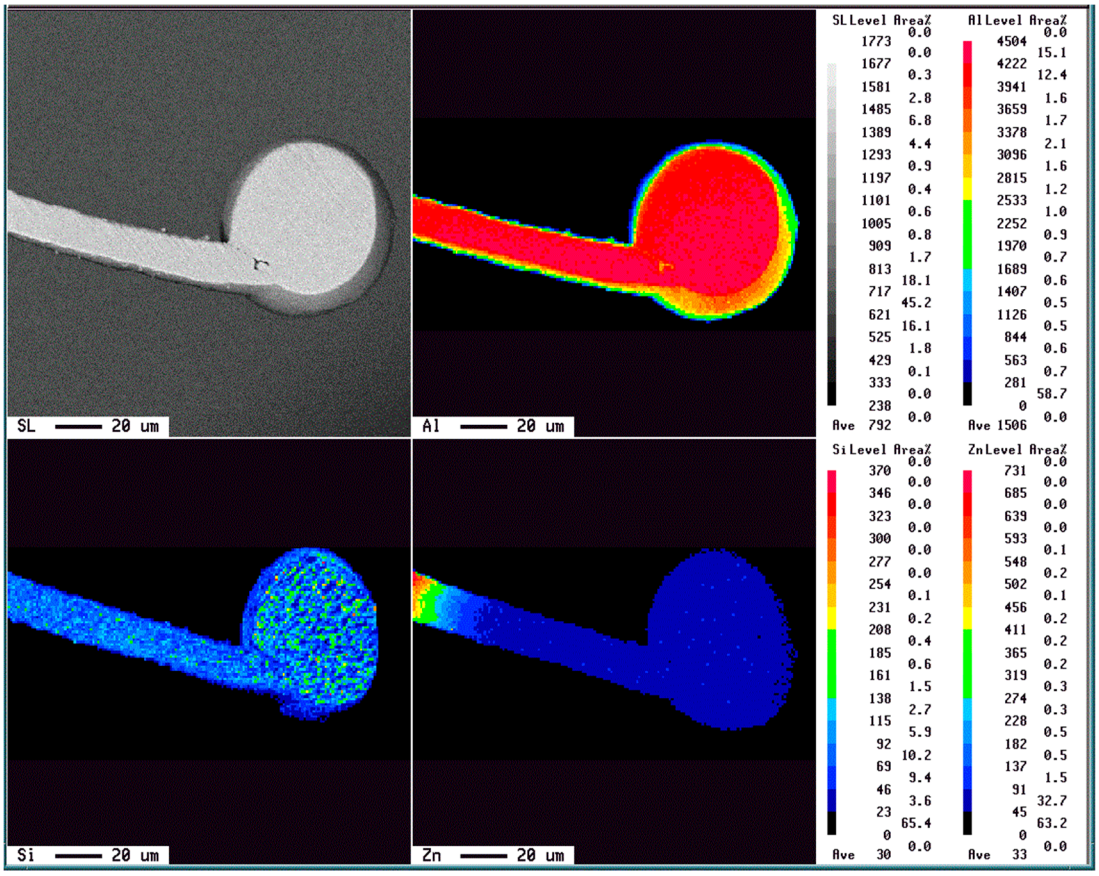

Figure 4 Electron probe X-ray micro-analyzer (EPMA) images of the ZAS250-FAB.

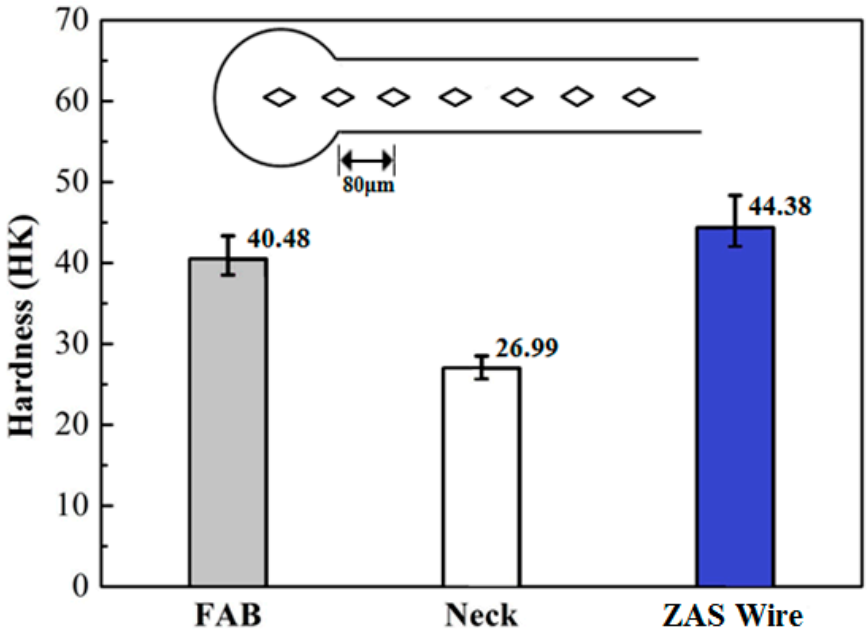

(a)

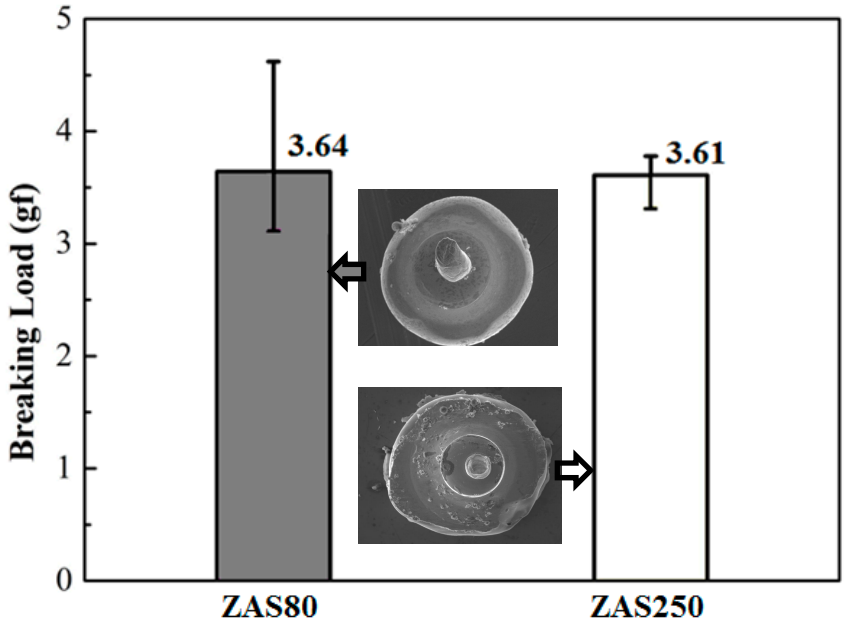

(b)

Figure 5 (a) Hardness of the ZAS80 wire. (b) FAB pull strength for ZAS80 and ZAS250 wires.

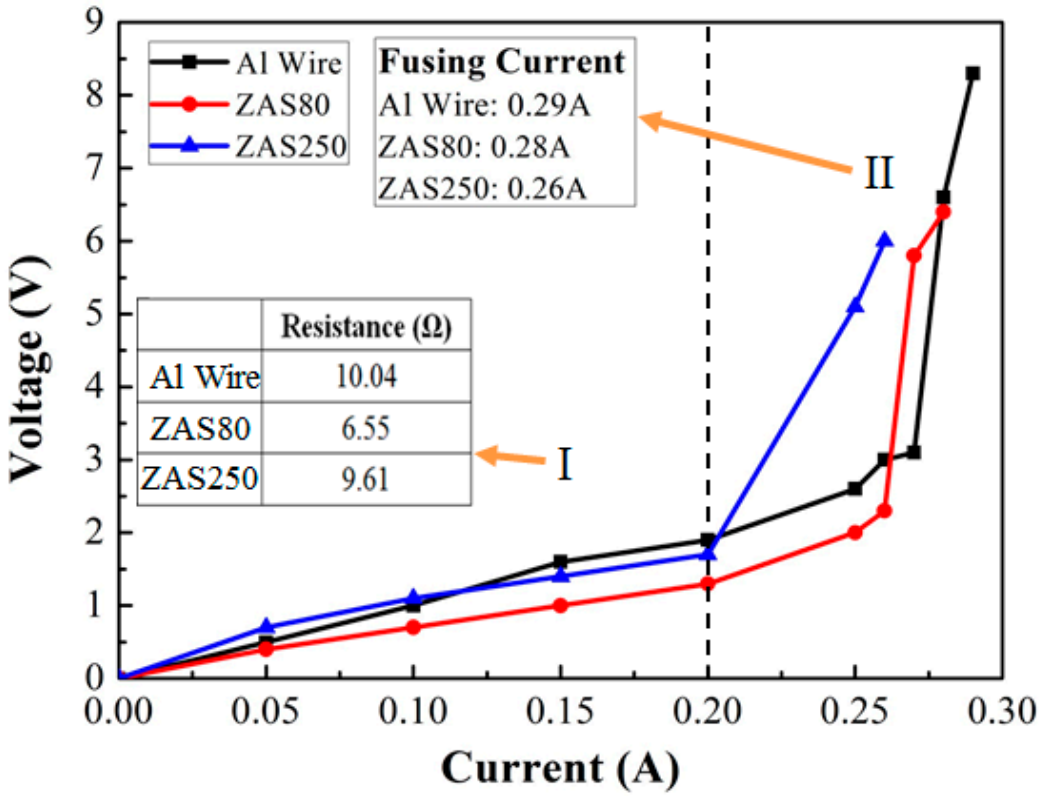

Figure 6 I-V curve and electrical properties of the three tested wires. Bare Al wire: wedge bonding. Coated Zn film (ZAS80, ZAS250) wire: ball bonding.

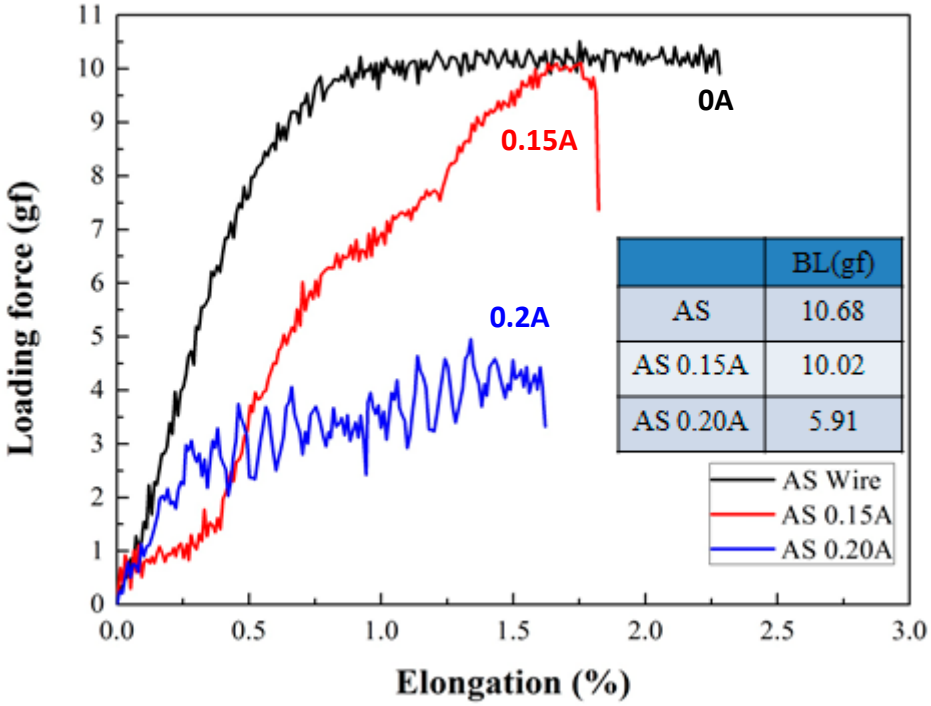

(a)

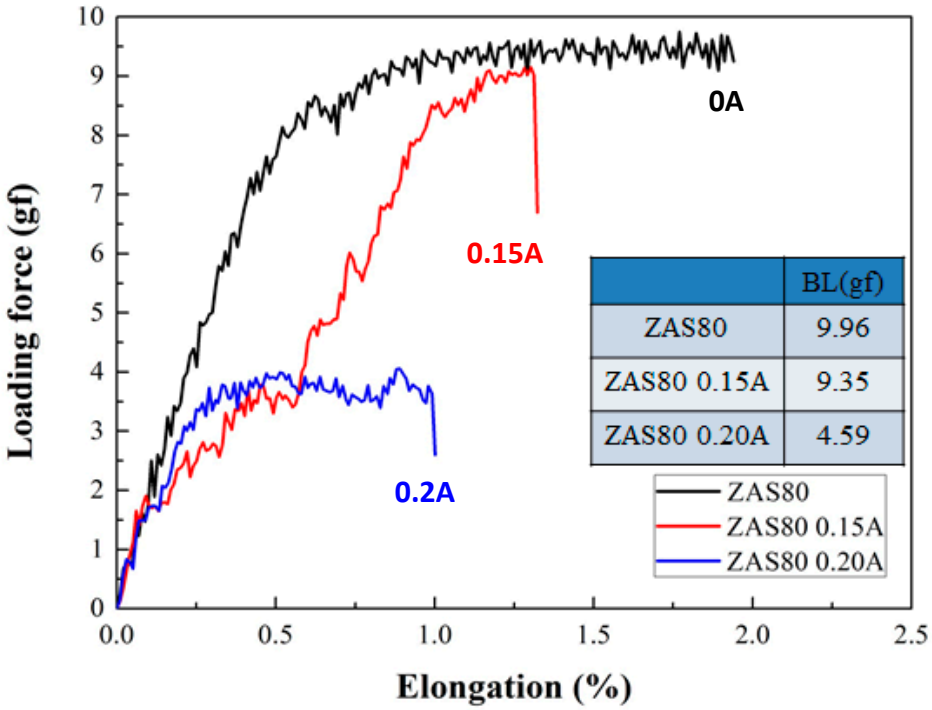

(b)

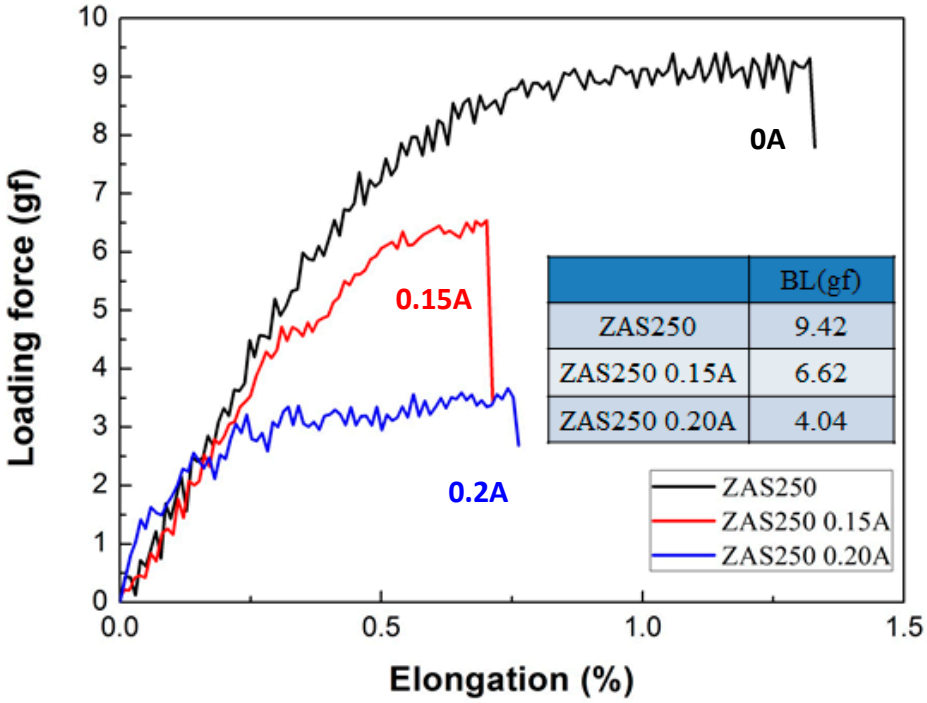

(c)

Figure 7 Bias-tensile curves of ZAS wires with different currents: **(a) un-coated Al-Si (AS), (b) ZAS80, and (c) ZAS250 wires.**

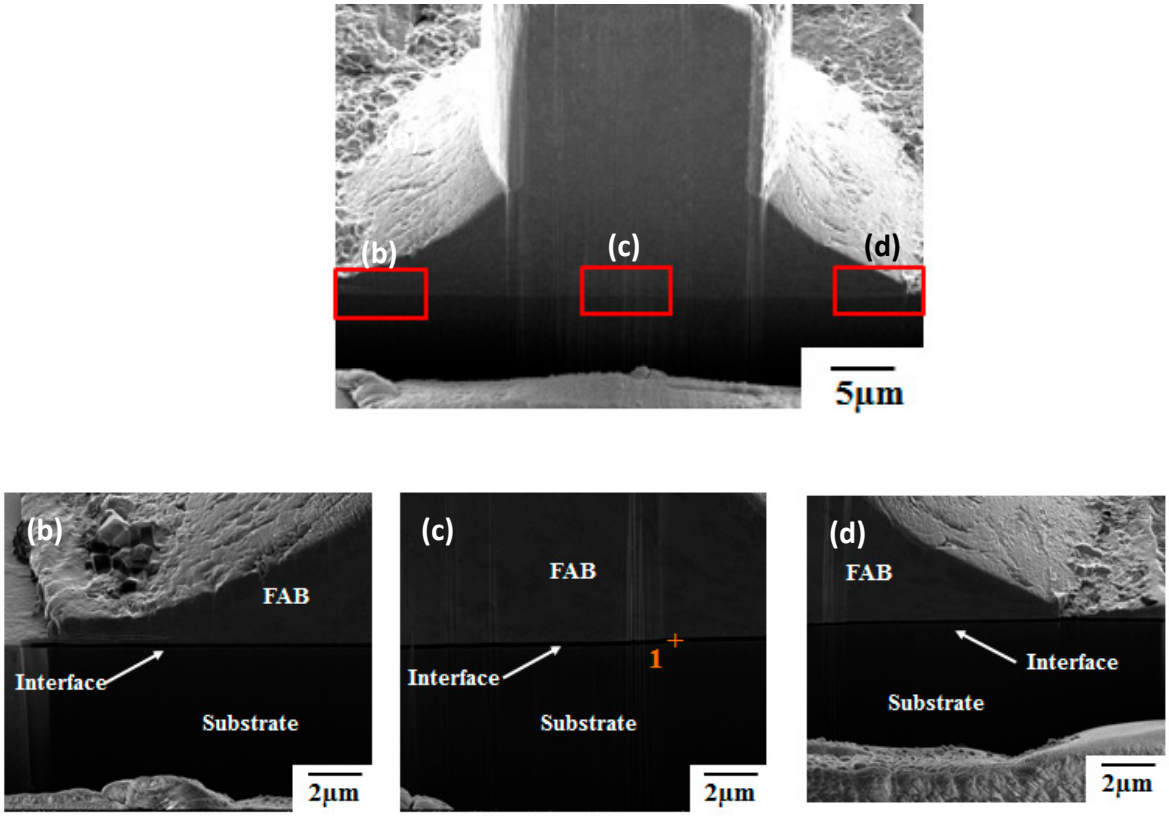

Figure 8 Bonding interface of ZAS80 wire: (a) interface characteristic, with (b), (c) and (d) being zoomed-in images of the red rectangles in (a). (1+ : no IMCs)

Preprints (www.preprints.org) | NOT PEER-REVIEWED | Posted: 18 November 2016 doi:10.20944/preprints201611.0100.v1

Peer-reviewed version available at Metals 2017, 7, , 152; doi:10.3390/met7050152

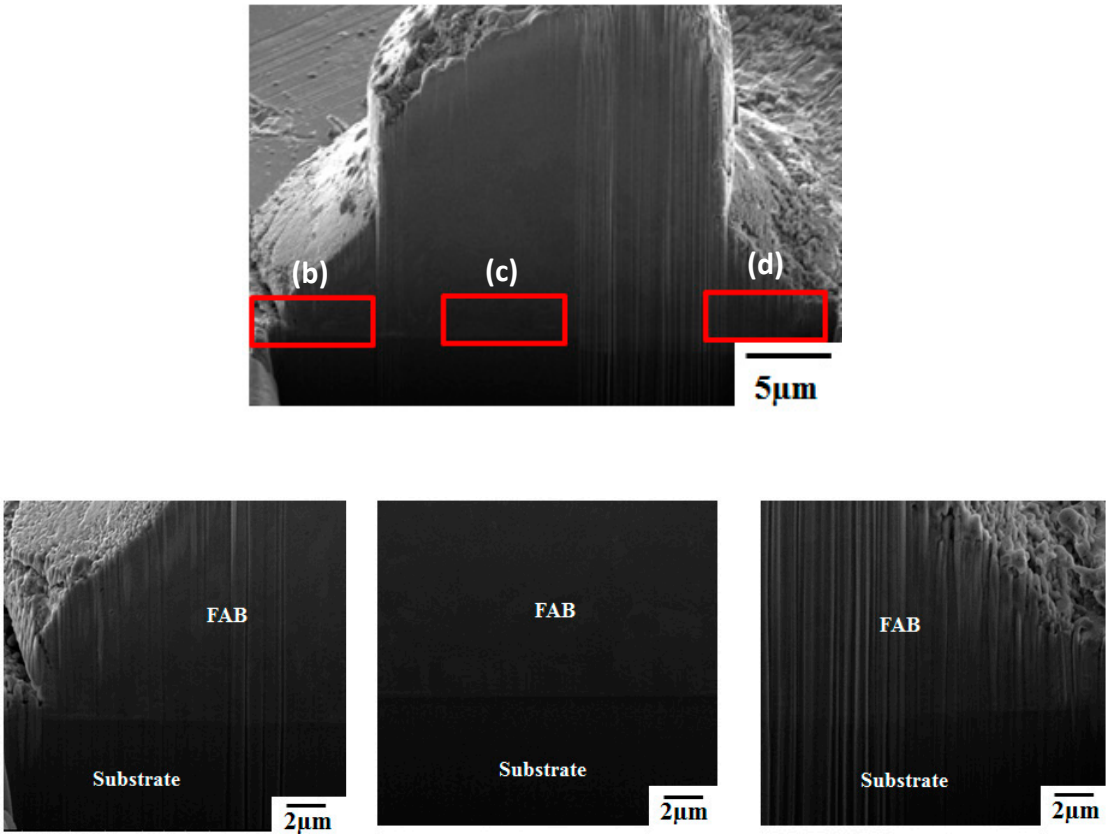

Figure 9 Bonding interface of ZAS80 wire with 60% fusing current for 24 hr: (a) interface characteristic, with (b) (c) and (d) being zoomed-in images of the red rectangles in (a).

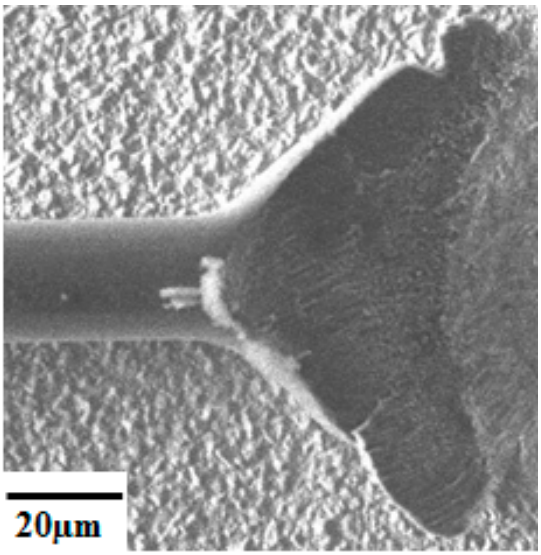

(a)

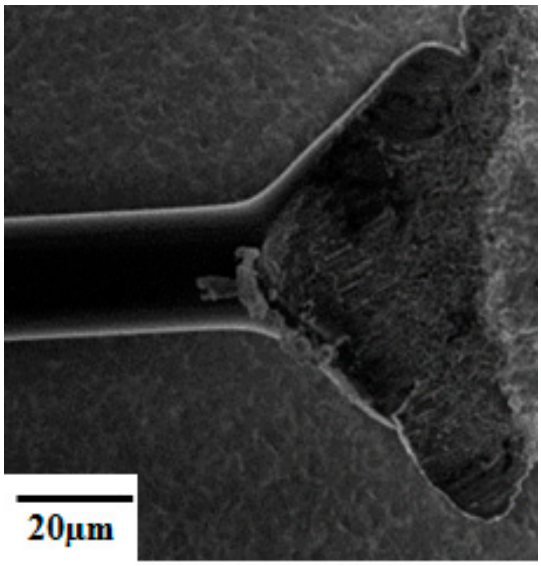

(b)

Figure 10 Surface of second bonding of un-coated Al-Si (AS) wire in vacuum: (a) before aging, and (b) after 48hr aging.

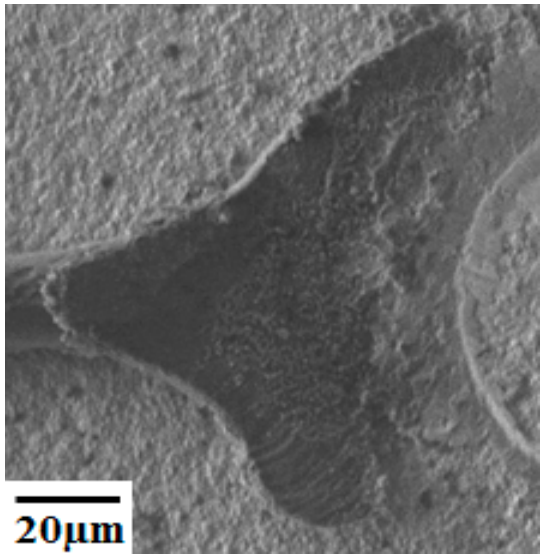

(a)

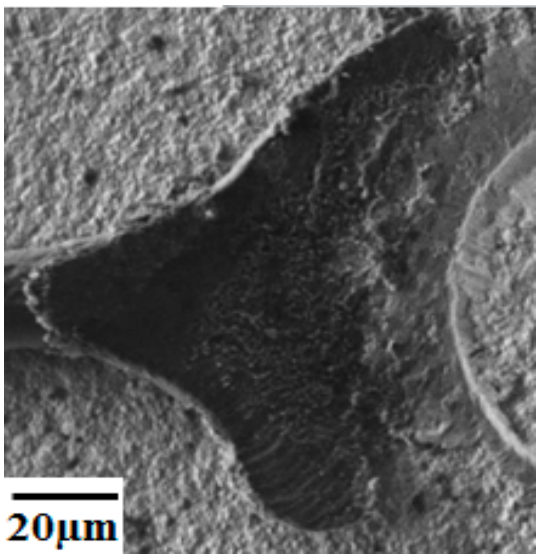

(b)

Figure 11 Surface of second bonding **of ZAS80 wire in vacuum: (a) before aging, and (b) after 48hr aging.**

Peer-reviewed version available at Metals 2017, 7, , 152; doi:10.3390/met7050152

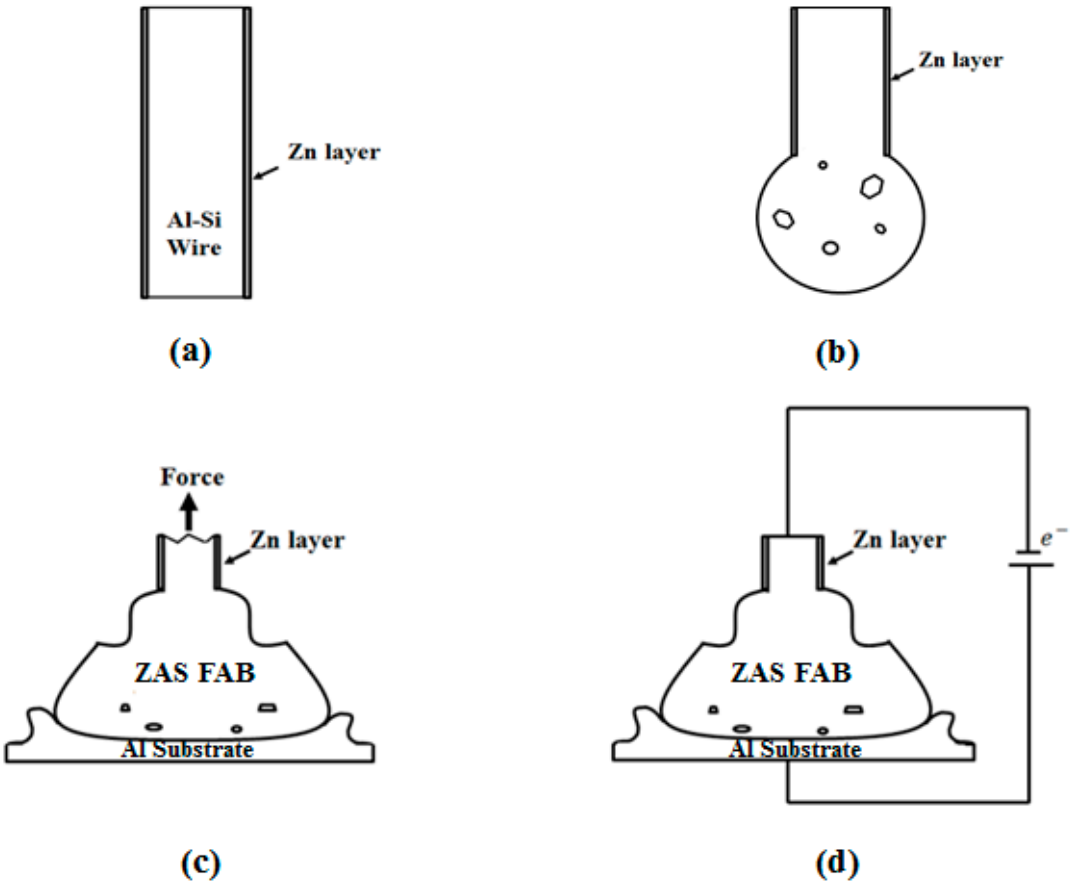

Figure 12 Mechanism of EFO and bonding: (a) ZAS wire, (b) ZAS FAB with micro voids, (c) bonding of FAB and fracture on neck zone after pull test, and (d) electrical properties test of the bonding structure.